

Controlled Recovery of Payloads at Large Glide Distances, Using the Para-Foil

C. F. KNAPP*

University of Notre Dame, Notre Dame, Ind.

AND

W. R. BARTON†

Sandia Laboratory, Albuquerque, N. Mex.

Recent progress of Sandia Laboratory in the development of a small guidance and control system and by the University of Notre Dame on the Para-Foil has indicated that the design of a system capable of recovering a 150-lb payload from altitudes greater than 300,000 ft and ranges of from three to five times the deployment height (60,000 ft) is quite feasible. The Para-Foil is a completely nonrigid, self-inflating flying wing, capable of being packed and deployed like a conventional parachute and able to glide large distances. The guidance package is an electromechanical control system employing a direction-finding antenna to control the direction of the Para-Foil's glide path with respect to a ground or shipboard transmitter. The recovery system design program includes such parameters as size and weight of the recovery unit, size of the payload (W/S wing loading), glide ratio and wind structure, and flare-out capabilities in the recovery area. The full-scale recovery program includes numerous packing, deployment, and glide tests. These tests demonstrated successful deployment, excellent gliding performance ($L/D = 3.88$) and dynamic flight stability, and very low impact velocities during the final recovery phases. Recent guidance and control tests also demonstrated excellent response in maneuverability of the Para-Foil. This paper summarizes the design program and the results of full-scale deployment and guided recovery flight tests and demonstrates the potential of the Para-Foil for use in many space-age recovery programs.

Nomenclature

AR	= aspect ratio (dimensionless)
b	= span, ft
C	= chord, ft
C_D	= drag coefficient (dimensionless)
C_L	= lift coefficient (dimensionless)
V_H	= horizontal velocity with respect to air, fps
V_h	= horizontal velocity, with respect to ground, fps
V_V	= vertical velocity, fps
W	= weight (payload), lbs
W_i	= wind velocity, ft/sec
W/S	= wing loading, lb/ft ²
x	= horizontal space coordinate fixed to earth, ft
X	= coordinate aligned with the velocity vector V , ft
z	= vertical space coordinate fixed to earth, ft
Z	= coordinate perpendicular to the velocity vector V , ft
α	= angle of attack, deg
γ	= glide angle, deg
γ_w	= glide angle with respect to ground, deg
ρ	= density, slugs/ft ³
ρ_o	= standard sea level density, slugs/ft ³
σ	= density ratio ρ/ρ_o (dimensionless)
λ	= wavelength, in.

Introduction

SINCE the middle of the 1940's, sounding rocket flights have been conducted in order to make observations of the earth's upper atmosphere. As the program progressed, in-

creasingly sophisticated equipment was incorporated into the launch vehicle, emphasizing the need for recovery of the payloads.

Heretofore, primary recovery has been accomplished by conventional parachutes which basically follow ballistic trajectories due to drag and gravity. However, because of the winds aloft, such a technique can cause large dispersion in the final impact area or even loss of the payload.

The recent development of the Para-Foil¹⁻¹⁰ now offers the possibility of a recovery system possessing large glide ratios in excess of 4 to 1. With a guidance and control system, the Para-Foil can deliver a payload from large distances to predetermined locations.

The launch and recovery operation is shown in Fig. 1. The launch vehicle carries the payload to an altitude of approximately 100 miles. The payload then follows a ballistic trajectory until an altitude of 60,000 ft where a small conventional drag chute will decelerate the payload to approximately 250 fps, at which time the Para-Foil system is deployed for the final controlled gliding phase. Figure 1 also illustrates the expected idealized glide path for the Para-Foil system under no-wind and head-wind conditions.

Description of the Para-Foil†

The Para-Foil is a flying wing with an airfoil section and a rectangular plan form (Fig. 2). It differs from the conventional wing in the very important feature that it is completely nonrigid and therefore can be packed and deployed like a conventional parachute. The Para-Foil obtains its rigid flight configuration from the ram air pressure entering the open leading edge and from the negative or reduced

Presented at the AIAA Sounding Rocket Vehicle Technology Specialist Conference, Williamsburg, Va., February 27-March 1, 1967 (no paper number; published in bound volume of meeting papers); submitted June 12, 1967; revision received September 27, 1967. This work was partially supported by the United States Atomic Energy Commission. The authors would like to express their gratitude to D. Jalbert, the inventor of the Para-Foil, and to J. Nicolaidis, Head of the Aero-Space Department, University of Notre Dame, who is the director of the Para-Foil Project, and to C. Coonce and W. Pepper of the Sandia Laboratory for their work on the testing and reporting phases of the program.

* Graduate Student, Department of Aero-Space Engineering.

† Supervisor, Rocket and Recovery Systems Division, Aero-Thermodynamics Department.

† The Parafoil was invented by D. Jalbert and is a proprietary product (patent 3285546) of Space Recovery Research Center Inc., Boca Raton, Fla. It was later learned that the name "Parafoil" had first been used by H. G. Geinrich of the University of Minnesota, for some of his parachutes; however, with his concurrence, the name "Para-Foil" or Jalbert Para-Foil, has been applied to the new designs.

pressures over the top cambered surface. It is actually composed of individual air cells connected by porous nylon cloth ribs to allow pressure equalization throughout the interior. The exterior, i.e., the side profiles, and top and bottom surfaces are made of a nonporous nylon fabric. Therefore, the air in each cell and in the Para-Foil as a whole is essentially stagnant.

The flares, or pennants, along the bottom surface serve a) to distribute evenly the payload forces along the bottom surface, b) to reduce aerodynamic losses at the sides of the unit, and c) to provide side area for obtaining dynamic flight stability. Turn control is accomplished by asymmetrically pulling on the outer rear shroud lines. Pitch control and flare out capabilities can be accomplished by an even pull on both lines. Furthermore, full-scale packing and deployment tests demonstrate that this new system can be deployed like a parachute and glide like a conventional rigid airplane wing.

Results of two years of research and development of the Para-Foil at the University of Notre Dame,[§] plus joint tests with Sandia Laboratory, the Air Force, and NASA, have yielded significant progress so that the full-scale guidance and control tests necessary for the recovery operation could be carried out. The design and testing of a special Para-Foil and the associated Sandia Laboratory guidance and control package are presented in the following sections.

Objectives of the Recovery Program

The goal of the sounding rocket recovery program is the controlled recovery of a 150-lb payload after separation from the booster system at altitudes of greater than 300,000 ft. The payload would decelerate to subsonic velocities (250 fps) after deployment of a small drag chute, at which time the

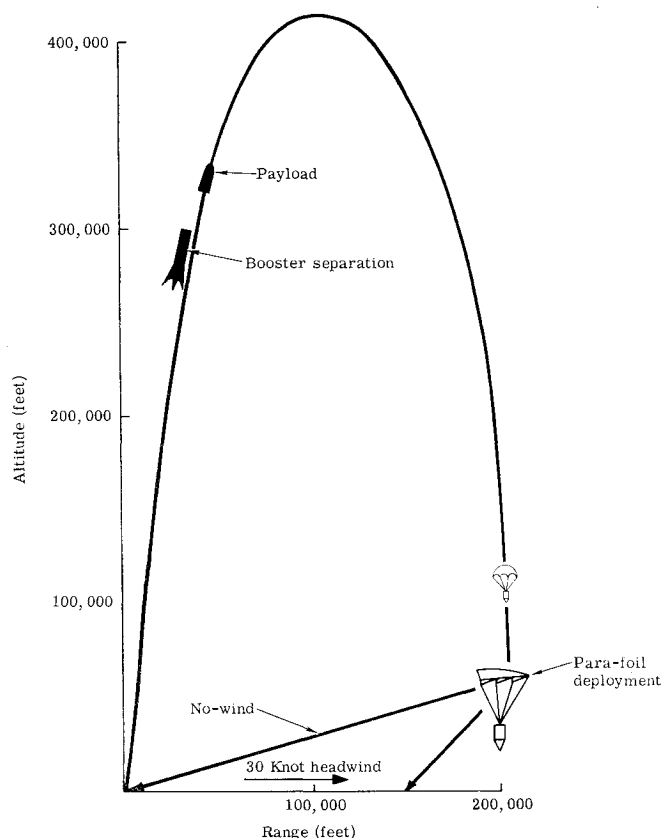


Fig. 1 Typical launch and recovery operation.

§ All of the research studies were performed with wind tunnel and full-scale Para-Foils provided by the Space Recovery Research Center Inc.

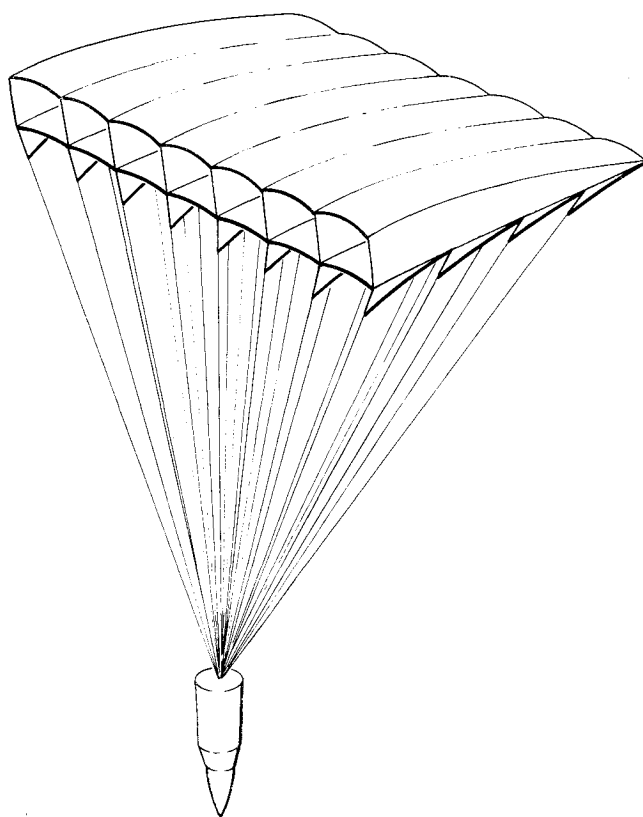


Fig. 2 Para-Foil attached to nose cone.

Para-Foil could be deployed (60,000 ft) for the final controlled glide phase to a predetermined recovery site.

The requirements¹⁰ for the gliding portion of the recovery operation are 1) the system must be able to penetrate a 30-knot head wind at sea level, while 2) maintaining a ground trajectory of at least 1 to 1, 3) with a rate of descent of 30 fps or less. The equations of gliding flight that follow will allow the construction of a set of Para-Foil design curves for the foregoing requirements.

Para-Foil Design Parameters

Gliding Flight

A Para-Foil in free gliding steady flight is shown in Fig. 3. From the equations for its motions the glide angle is given by

$$\gamma = \tan^{-1} \frac{1}{L/D} \quad (1)$$

This is the classic equation for the aerodynamic efficiency of gliding flight. The higher the L/D ratio, the smaller the

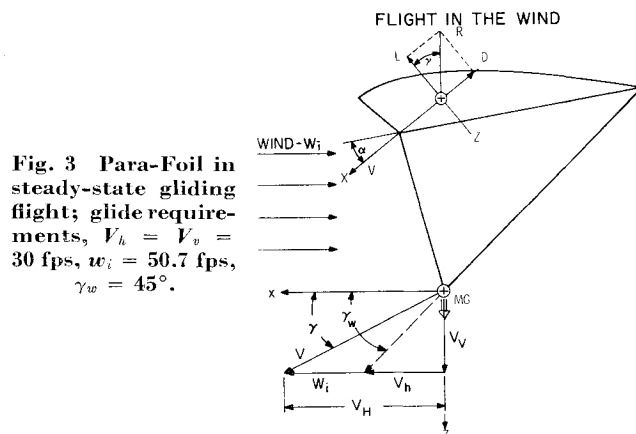


Fig. 3 Para-Foil in steady-state gliding flight; glide requirements, $V_h = V_v = 30$ fps, $w_i = 50.7$ fps, $\gamma_w = 45^\circ$.

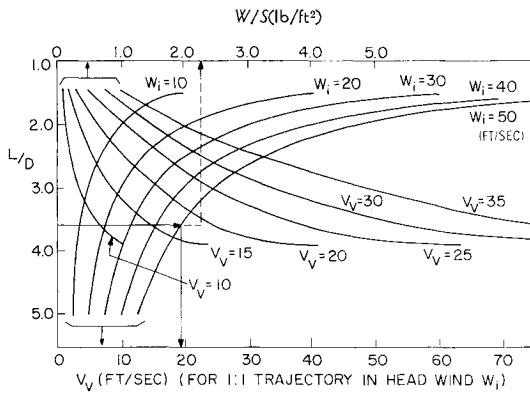


Fig. 4 Para-Foil gliding flight design curves; $\alpha = 0^\circ$ – 10° .

glide angle and, of course, the greater the gliding range. It is important to notice that Eq. (1) is independent of the weight.

The velocity of the Para-Foil in gliding steady flight is

$$V = [2MG/\rho S(C_L \cos \gamma + C_D \sin \gamma)]^{1/2} \quad (2)$$

$$V \approx [(2/\rho C_L)(W/S)]^{1/2} \quad \text{for small } \gamma \quad (3)$$

Also, the horizontal and vertical components of velocity may be computed from

$$V_H = V \cos \gamma \quad (4)$$

and

$$V_V = V \sin \gamma \quad (5)$$

Gliding Requirements

One of the most important parameters required in the recovery operation is the wind-penetration ability of the system. The requirement for wind penetration is that the Para-Foil must maintain a $\gamma_w = 45^\circ$ in a 30-knot (50.7 fps) head wind while maintaining a rate of descent of 30 fps or less at sea level. This requirement may now be investigated by using the concepts already developed. Using Fig. 3 it is seen that the horizontal velocity of the Para-Foil must be at least $V_H = 80.7$ fps. The total flight velocity must be at least $V = [80.7^2 + 30^2]^{1/2} = 86.1$ fps. In addition, from Fig. 3, and using Eq. (1), the minimum required L/D ratio must be 2.69; i.e.,

$$L/D = \frac{1}{\tan \gamma} = \frac{1}{30/80.7} = 2.69$$

Furthermore, the gliding performance of the Para-Foil is the same in a steady wind as in the no-wind condition. However, the Para-Foil's ground speed changes with the wind condition. Figure 3 represents this wind condition. Thus, to an observer on the ground, the glide angle γ_w is quite different under different wind conditions.

The glide angle which a ground observer would see is given as

$$\gamma_w = \tan^{-1}[V_V/(V_H - W_i)] \quad (\text{head-wind case}) \quad (6)$$

It is readily seen that the Para-Foil would make no headway into the wind if $W_i = V_H$. Therefore, the ability of the Para-Foil to glide into a strong wind requires large velocity and small γ . This means that a large wing loading (W/S), Eq. (3), and a good L/D ratio, Eq. (1), are desired.

General Glide Angle Formula for $\gamma_w = 45^\circ$

With the requirement that $\gamma_w = 45^\circ$, V_h can be set equal to V_V , Fig. 3, from which it is seen that

$$\tan \gamma = V_V/(W_i + V_V) \quad (7)$$

However, substituting Eq. (1) into Eq. (7),

$$\frac{V_V}{W_i + V_V} = \frac{1}{(L/D)} \quad (8a)$$

is obtained, from which rate of descent is obtained as

$$V_V = \frac{W_i}{(L/D) - 1} \quad (8b)$$

This equation satisfies the mission requirement for $\gamma_w = 45^\circ$ and allows the determination of the necessary L/D and rate of descent for any particular value of the head wind. Values of the variables L/D , V_V , W_i , and W/S are plotted in Fig. 4. As before, for a head wind of 30 knots (50.7 fps) and a rate of descent of 30 fps, the required value of L/D is 2.69. Equation (9), however, is a general equation that enables the consideration of any wind, any rate of descent, and any L/D ratio for which $\gamma_w = 45^\circ$.

Wing Loading Requirements

Thus far, the wing loading required to produce the necessary total velocity (of at least 86.1 fps) for a given L/D ratio has not been considered. The wing loading is found from Fig. 3 to be

$$\frac{W}{S} = \frac{C_L \rho}{2 \cos \gamma} V^2 = \frac{C_L \rho}{2 \cos \gamma} [V_V^2 + (V_V + W_i)^2] \quad (9)$$

Substituting Eq. (8a) yields

$$W/S = (C_L \rho V_V^2 / 2 \cos \gamma) [1 + (L/D)^2] \quad (10)$$

This is the second basic equation used in the Para-Foil system design to satisfy the mission requirement. Since C_L , L/D , and γ are functions of α , then C_L , γ , and α may be expressed as functions of L/D .

The necessary wing loading may be computed from Eq. (10) for the values of V_V and L/D found from Eq. (8b) for a particular head wind, and for ρ . Once the wing loading is known, the area of the Para-Foil required to carry the payload may be determined.

To summarize, Eq. (8b) and Eq. (10) serve as the two basic equations for Para-Foil design. Once the aerodynamic characteristics of the Para-Foil are known, the basic design charts based on these equations can be prepared and the special Para-Foil area selected. Also, for a given area of the Para-Foil the "off-design" performance can be computed from these same general equations.

Aerodynamic Characteristics[¶]

From wind-tunnel and full-scale free flight tests of various Para-Foil configurations, Para-Foil model 125 was chosen as the best unit for the recovery operation. The airfoil profile of model 125 is presented in Fig. 5. This unit has a maximum thickness of 21.5% at 0.25% chord.

The aerodynamic characteristics for this unit, C_L , and L/D , which are needed for the design equations, are presented in Figs. 6 and 7. These data were obtained from wind-tunnel tests of small models, both rigid and nonrigid, and gliding tests for L/D values of full-scale models. These curves have been adjusted for the proper aspect ratio and Reynolds number of the Para-Foil under consideration, and are believed to represent a conservative estimate of the aerodynamic characteristics of the full-scale model 125 in free gliding flight. Details of the wind-tunnel testing procedure and the full-scale free flight test program are presented in Ref. 6.

[¶]Subsequent to the preparation of this paper, full-scale Para-Foils of $AR = 2.0$ and 2.5 have been successfully flight tested, also wind-tunnel models of $AR = 3$ have been tested. Substantial improvements in lift curve slope and L/D have been obtained.

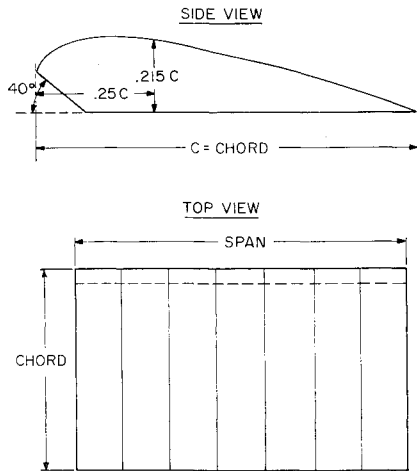


Fig. 5 Para-Foil design, model 125.

Mission Design Curves

The aerodynamic data for the Para-Foil may now be substituted into Eq. (10) and the basic Para-Foil design curve prepared. Actually, two curves are prepared since there are two angles of attack at which the same L/D ratio can be obtained. One curve is for $\alpha \leq 10^\circ$ and the other for $\alpha \geq 10^\circ$ (not shown). Figure 4 may now be used to determine the area of the Para-Foil required to satisfy the mission specifications for various combinations of L/D , V_v , and W_i .

From Fig. 4 it is seen that for a Para-Foil with an L/D of 3.6 entering a 30-knot (50.7-fps) wind, the vertical velocity (V_v) will be 19.5 fps (solid line). For this value of V_v the required wing loading W/S is 2.25 lb/ft² (dotted line). The curves at sea level are used since the W/S for wind penetration is the most critical. For example, at 60,000 ft a Para-Foil with the same L/D and W/S can penetrate a head wind (W_i) of 163 fps and maintain a 1:1 trajectory. The W_i at any altitude is the W_i at sea level divided by the density ratio (σ) at that altitude. Thus, a Para-Foil with a W/S of 2.3 and an area of 65.6 sq. feet is required.

Recommended Aspect Ratio (Span/Chord)

Parameters that must be taken into account in choosing the aspect ratio are the aerodynamic efficiency (L/D) and the payload location⁸ to insure proper inflation. Ideally, very large aspect ratios would be preferred in order to obtain large values of L/D . However, for the case of the Para-Foil, this is not always practical. Since the Para-Foil is a completely

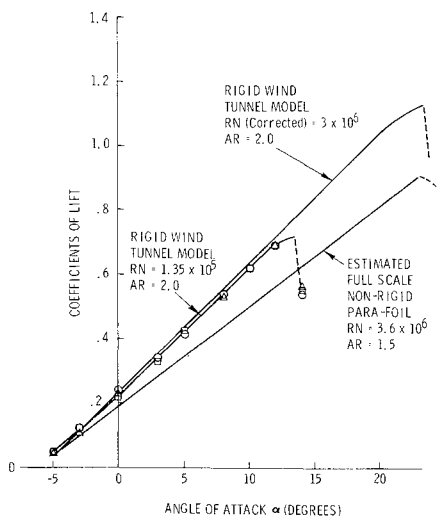
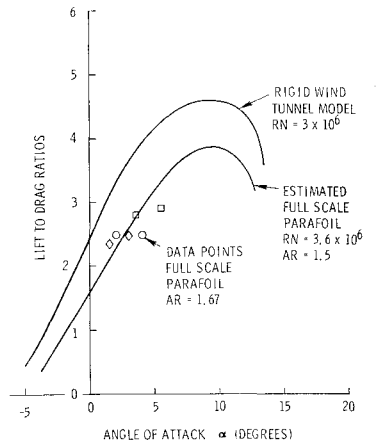


Fig. 6 C_L vs α for Para-Foil model 125.

Fig. 7 L/D vs α for Para-Foil model 125.



nonrigid system and dependent upon the dynamic pressure for its inflation, it is of prime importance that the payload be located at the proper position below the bottom surface to insure proper inflation.

In order to achieve a conservative design and insure spanwise rigidity, an aspect ratio of 1.5 was selected for the recovery Para-Foil. Such an aspect ratio is considered conservative for safe deployment, good aerodynamic efficiency, and excellent flight stability. A summary of the design data for the recovery Para-Foil is listed in Fig. 8.

Guidance Package Design

A block diagram of the control system for the automatic parachute guidance unit is shown in Fig. 9. The basic system consists of 1) a ground transmitter, 2) a specially designed receiving antenna, 3) a receiver capable of AM reception, 4) a reference oscillator, 5) a comparison circuit to operate the proper control relay, and 6) a motor to drive the control line of the parachute.

The system is designed to keep the unit pointed toward an unmodulated transmitter by using the receiver antenna pattern to determine the proper direction of control. The reference oscillator drives the antenna switching network at 1-kHz. The switching network thus allows the receiver to receive the rf signal from each antenna one-half of the time at a rate of 1-kHz. The receiver output is amplified by an audio amplifier and is then fed to a comparison circuit. The comparison circuit switching transistors are switched by the same 1-kHz oscillator used with the antenna switching network. The voltage difference is detected by the comparison circuit. When a difference exists, there will be an output to close a control relay to the control motor, to drive the control lines of the Para-Foil. When no voltage difference exists, neither control relay is closed. Thus, when the unit revolves

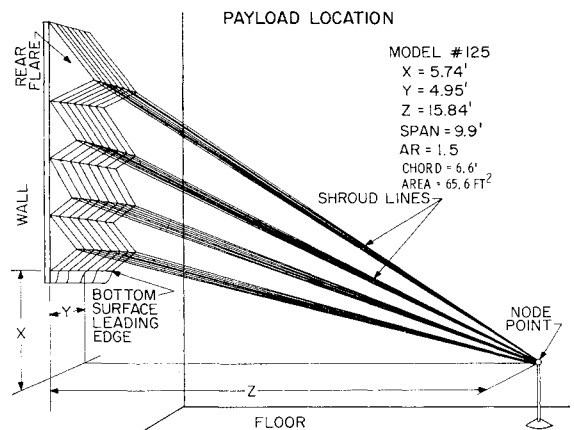


Fig. 8 Para-Foil nodal point rigging diagram.

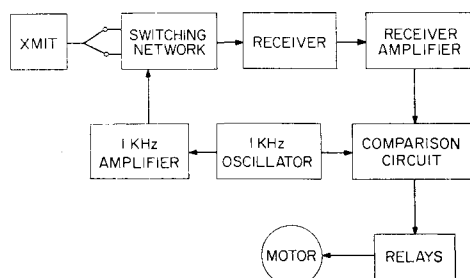


Fig. 9 Control system block diagram.

to either side of the desired flight path, the antenna closest to the transmitter will have a larger rf signal, and a voltage difference is provided to operate the control lines to drive the unit back to the null position.

Receiver Antenna

One method of obtaining guidance information is to utilize the horizontal radiation pattern of two vertical antennas. Terman¹¹ shows that with appropriate spacing and phasing, a cardioid pattern can be obtained. Also if the feedpoint is switched from one antenna to the other, the cardioid pattern is reversed. A combination of these patterns will then have two crossover points of equal signal voltage. Guidance information can then be obtained by comparing the difference in signal levels between the two patterns as they are alternately switched. The problem of finding the optimum phasing and spacing for high signal level and a steep slope at the pattern cross-over points was simplified by using the data in Ref. 12.

The antenna parameters are as follows:

length of antenna elements = 7.375 in.
 spacing of antenna elements = 4.250 in.
 diameter of ground plane = 12 in.
 length of phasing line = 0.20λ

The antenna system has a 2.8 to 1 voltage standing wave ratio when measured at the base of the antenna. By use of a $\lambda/4$ 35-ohm transformer, this was improved to 1.7 to 1. A more complete description of the control system is contained in Ref. 13.

Control of Para-Foil

Control of the Para-Foil is achieved by pulling on shroud lines attached to flares in the rear corners. The number of flares used depends upon the length of control line, travel of the guidance system, and the control response time desired. It was found for this control unit that a group of four lines on each side consisting of two outboard trailing lines and the two lines in front of these provided the most effective control.

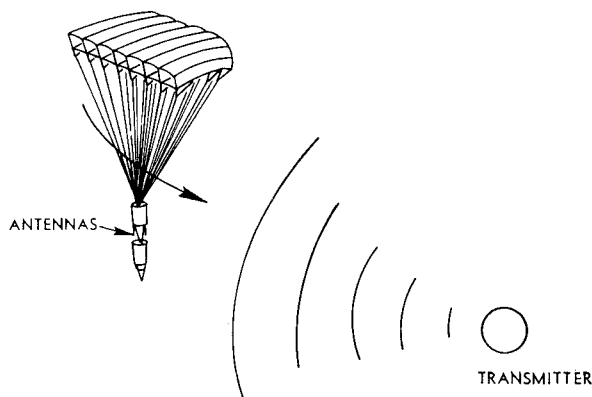


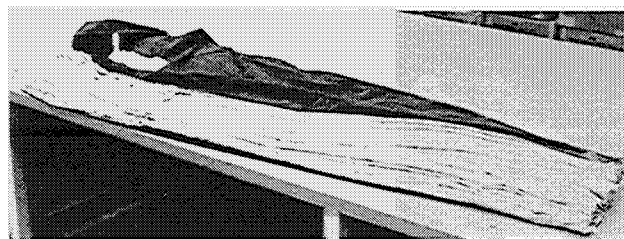
Fig. 10 Para-Foil guidance sequence.

The maneuverability of the Para-Foil is accomplished by pulling on one of the two sets of control lines. A pull on the right set causes the unit to bank to the right, whereas a pull on the left causes a bank to the left. With this type of control, lift is lost on the side deformed by the pull of the control line. Therefore, control of this Para-Foil is produced by a "spoiler effect" as opposed to the conventional aileron effect.

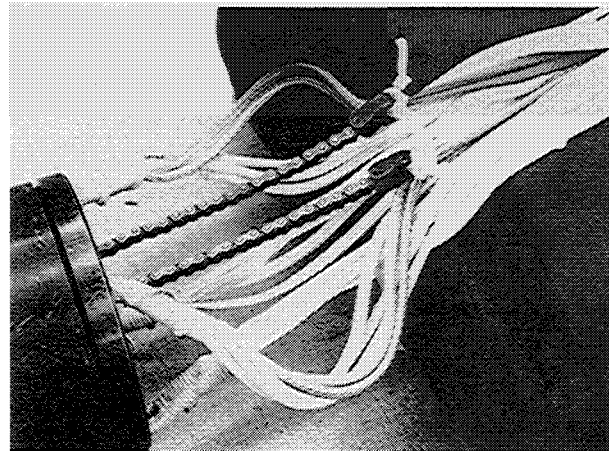
This method of control, therefore, necessitated that the control unit be attached to the Para-Foil so that the antenna nearest the transmitter will cause the chain on its side to be pulled down and thereby initiate a turn toward the transmitter. The attachment of the guidance package and the control sequence are illustrated in Fig. 10.

Flare-Out Capabilities

The ability of the Para-Foil to flare out upon landing has been demonstrated very successfully in manned flights. By pulling simultaneously on both control lines at about 5 to 10 ft from the ground the jumper can abruptly increase the lift and drag and thereby slow the vertical and forward speeds of the Para-Foil to values which will allow a standup landing.



a) Accordion-folded, Para-Foil canopy



b) Para-Foil suspension line attachment to guidance package, showing guidance chain



c) Packed Para-Foil

Fig. 11 Para-Foil packing procedure.

The same control maneuver can be accomplished in the unmanned system by causing an abrupt simultaneous pull on the control lines of the guidance package or by a change in the center of gravity of the system, i.e., by shifting the payload. Either of these methods can be accomplished by conventional sensing or pyrotechnique devices.

At the present time flare-out capabilities have not been built into the guidance systems since the payloads have successfully withstood the landings of the preliminary tests. However, for more optimum and complex recovery requirements, flare-out upon landing may be desirable.

Para-Foil Packing and Deployment Procedures

Full-scale tests demonstrated the Para-Foil's capability for successful deployment from the packed condition. Preliminary tests were carried out on numerous full-scale Para-Foils (six designs) at Notre Dame University and at Sandia Laboratory. These drop tests were conducted from aircraft (15 drops), helicopter (16 drops), and from tethered units (numerous), at altitudes ranging from 50 to 3000 ft. More recently, successful drop tests have been carried on by the Air Force at Wright Field, and in a new series by Sandia Laboratory.

A very successful packing technique has been developed by Sandia in conjunction with the Kirtland Air Force Base Prototype Packing Facility. Two packing methods have been used and found to give reliable deployment. The first method consists of a series of light line ties which insure orderly deployment of the accordion folded lines and canopy. The second method presently being used is a deployment sleeve into which the spanwise accordion folded canopy, Fig. 11, is inserted. The sleeve is then accordion folded chordwise and inserted in a cylindrical bag with canopy locking flaps to insure lines-first deployment. The sleeve method is similar to that used with personnel parachutes.

Flight Test Results

Deployment

Numerous tests to develop packing procedures for reliable deployment and inflation have been made. These tests have shown that several packing techniques can be used, two of which are presented, and that the deployment of the Para-Foil is extremely reliable.

Glide Ratio (L/D)

Tests to obtain L/D values on full-scale free gliding Para-Foils have been carried out at the University of Notre Dame. L/D values of 2.9 at $\alpha = 5^\circ$ on model 125, $AR = 1.67$, have been obtained. This same model was then tested at Sandia Laboratory's Tonopah Test Range (TTR), Tonopah Nev., on May 6, 1966. This test¹⁴ had full cinetheodolite camera

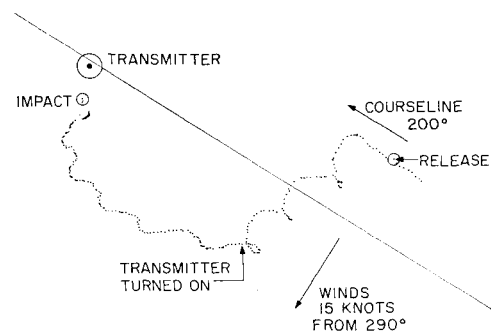


Fig. 13 Radar plot of a side-wind controlled flight (1 in. = 1000 ft).

coverage. The average L/D for this flight, subtracting the winds, was 3.88. This higher L/D ratio is probably due to a higher trim α as can be seen from Fig. 7. The L/D values from these tests demonstrates the ability of the Para-Foil to successfully meet the gliding requirement.

Controllability

Of particular importance were the guidance and control tests by the Sandia Laboratory. During the week of October 17, 1966, guidance tests were conducted at TTR, using the standard Sandia Laboratory guidance package. Adequate control and proper guidance are shown in the two radar plots of Figs. 12 and 13. In Fig. 12, Para-Foil ($AR = 1.86$) with a wing loading of 1.4 was dropped at an altitude of 5120 ft abs. and a downwind range of 6500 ft. This Para-Foil was guided to within 1800 ft of the transmitter while penetrating a 21-knot head wind. This results in a 1:1 trajectory for a 21-knot head wind and a wing loading of only 1.4.

Figure 13 is the radar plot for the cross wind condition. The same system was released at an altitude of 4200 ft abs. and a range of 5000 ft. During this test, the guidance and control transmitter was not turned on until later in the flight (Fig. 13). As can be seen in the plot, at that time the Para-Foil then homed on the transmitter and landed only 600 ft away. The results of these preliminary tests confirm the capability of the Sandia Laboratory guidance system and the Para-Foil to be successfully controlled and guided to a predetermined location.

Future Plans

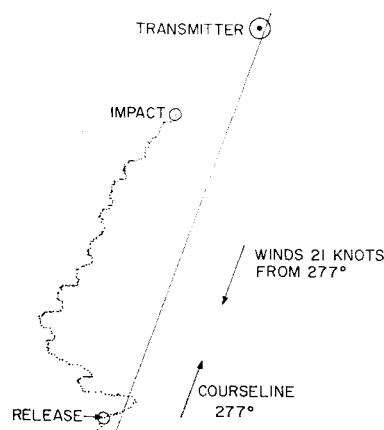
Plans are under way to further optimize the guidance package performance and to reduce its size by the use of integrated circuits. A new test vehicle is being designed and fabricated to allow the guided Para-Foil system to be carried by any fighter aircraft with 14-in. lug spacing on an external pylon. The test vehicle is identical with Sandia Laboratory's Nike-Tomahawk payload, except for the addition of lugs and fins for aircraft carriage and safe release and separation. This vehicle will contain a telemetry package to measure the opening and initial deceleration characteristics of the Para-Foil. The antenna signal strength and operating characteristics of the guidance package will also be telemetered during flight.

Future test plans include high-altitude, high Mach number tests and low-altitude, high dynamic pressure tests with and without the guidance package. Upon the successful completion of the flight test program, the Sandia Para-Foil recovery system will be used to return the payload from a high-altitude Nike-Tomahawk rocket flight.

References

- 1 Nicolaidis, J. D. and Knapp, C. F., "A Preliminary Study of the Aerodynamic and Flight Performance of the Para-Foil," *Conference on Aerodynamic Deceleration*, July 8, 1965, University

Fig. 12 Radar plot of a head-wind controlled flight (1 in. = 1000 ft).



of Minnesota; also reprint, Univ. of Notre Dame, Notre Dame, Ind.

² Nicolaides, J. D., "On the Discovery and Research of the Para-Foil," *International Congress on Air Technology*, Nov. 1965, Little Rock, Ark.; also reprint, Univ. of Notre Dame, Notre Dame, Ind.

³ Nathe, G. A., Knapp, C. F., and Nicolaides, J. D., "The Para-Foil and Targetry Applications," Feb. 8, 1966, Target Systems Planning Group, Hill Air Force Base, Ogden, Utah.

⁴ Nathe, G. A., "An Analysis of the Para-Foil," *AIAA Student Journal*, Vol. 5, No. 1, Feb. 1967, pp. 4-9.

⁵ Knapp, C. F., Nathe, G. A., and Nicolaides, J. D., "Launching Technique for Tethered Para-Foils," Manual, May 9, 1966, NASA, Cape Kennedy, Fla.

⁶ Nathe, G. A., Knapp, C. F., and Hall, C. R., "Wind Tunnel and Free Flight Testing of Para-Foil Number 125," Departmental Paper, June 1, 1966, Aero-Space Engineering Dept., Univ. of Notre Dame, Notre Dame, Ind.

⁷ Nathe, G. A. and Knapp, C. F., "A Qualitative Discussion of the Lateral-Directional Stability of Tethered and Towed Para-Foils," Departmental Paper, June 6, 1966, Aero-Space Engineering Dept., Univ. of Notre Dame, Notre Dame, Ind.

⁸ Gorin, B. F., "An Approximation of Spanwise Para-Foil Collapse," Departmental Paper, June 1966, Aero-Space Engineering Dept., Univ. of Notre Dame, Notre Dame, Ind.

⁹ Nicolaides, J. D., Nathe, G. A., and Knapp, C. F., "A Summary of the Tests Conducted on the Para-Foil," June 8, 1966, Aero-Space Engineering Dept., Univ. of Notre Dame, Notre Dame, Ind.

¹⁰ Nicolaides, J. D. and Knapp, C. F., "Para-Foil Design," UNDAS-866 JDN Rept., Contract AF 33(615)-5004, Aug. 1967, U.S. Air Force Flight Dynamics Lab., Wright Patterson Air Force Base, Ohio.

¹¹ Terman, F. E., *Radio Engineers Handbook*, McGraw-Hill, New York, 1943.

¹² "Ground Base VHF Automatic Direction Finder Equipment," Final Engineering Rept., Contract AF-08(606)-364, Aug. 1954, College of Engineering, Univ. of Florida, Gainesville, Fla.

¹³ Kane, M. T., Dicken, H. D., and Buehler, R. C., "A Homing Parachute System," SC-4537(RR), Jan. 1961, Sandia Corp., Albuquerque, N.Mex.

¹⁴ Coonce, C. A., "Para-Foil Free-Flight Test Data, SCTM 66-2616, Dec. 1966, Sandia Lab., Albuquerque, N.Mex.

MARCH-APRIL 1968

J. AIRCRAFT

VOL. 5, NO. 2

Some Contributions on a Control-Surface Buzz at High Subsonic Speeds

YASU HARU NAKAMURA*

National Aerospace Laboratory, Tokyo, Japan

A type of control-surface buzz occurring at high subsonic speeds where the shock waves form upstream of the flap is investigated. Experiments are made with a two-dimensional, airfoil-flap combination model at Mach numbers ranging from 0.78 to 0.81. First, measurements are taken of the amplitudes of the flap angle at the limit cycle of buzz and of the unsteady aerodynamic hinge moment for small oscillations using a free oscillation method. Second, optical observations of the flow around the model during the growth of buzz are made by means of a high-speed schlieren cinematography. The effects of frequency parameter and Reynolds number on the buzz characteristics are studied. It is shown that the separated flow behind the shock is responsible for the onset of the instability. On the basis of the present experimental results, a semi-empirical method of obtaining the unsteady pressure distribution over the surface of an airfoil at high subsonic speeds including shock wave is discussed and a possible mechanism of the onset of buzz is proposed. Furthermore, a method depending on the use of an air jet issuing from the upper surface of the airfoil was successfully devised in order to prevent the onset of this type of instability.

Nomenclature

a_1 = local speed of sound immediately upstream of shock
 c, c_F = chord length of airfoil and flap
 h_β = aerodynamic stiffness derivative of unsteady hinge moment $[= \rho V^2 c_F^2 (h_\beta + i\nu h_\beta) \beta e^{i\omega t}]$
 $-h_\beta$ = aerodynamic damping derivative of unsteady hinge moment

H = total unsteady hinge moment derivative vector $= h_\beta + i\nu h_\beta$
 H_o = unsteady hinge moment derivative vector for hypothetical nonseparated flow
 ΔH = incremental hinge moment derivative vector due to flow separation
 $|\Delta H|$ = magnitude of ΔH
 H_o = stagnation pressure of freestream
 M_1 = local Mach number of flow immediately upstream of shock
 M = Mach number of freestream
 p_o = static pressure of shock-free distribution at mean position of shock
 p_1, p_2 = static pressures of flow immediately upstream and downstream of shock
 R = Reynolds number based on chord length of airfoil
 t = time
 u_s = velocity of forward movement of shock
 V = air velocity
 x, x_s = distance along chord from leading edge
 β = flap angle

Received June 5, 1967; revision received September 11, 1967. This paper is an extract from part of the author's doctoral thesis submitted to the University of Tokyo. The author is indebted to R. Kawamura, K. Washizu, and J. Shioiri, University of Tokyo, for their criticism, helpful guidance, and encouragement during the course of the research. The experimental work was carried out at the Aerodynamics Division, the National Physical Laboratory, England, with the collaboration of L. Woodgate, while the author stayed at the NPL in 1964-1965 as a guest worker. The author also wishes to thank L. Woodgate, N. C. Lambourne, and H. H. Pearcy of NPL for their cordial assistance and valuable discussions in completing this paper.

* Research Engineer, First Airframe Division.